Analysis of Weakly Nonlinear Evolution Characteristics of Flow in the Constant Curvature Bend

Bin Li[2], Haijue Xu[1,2,*], Yuchuan Bai[1,2] and Ziqing Ji[2]

[1] *Skate Key Laboratory of Hydraulic Engineering Simulation and Safety, Tianjin University, Tianjin 300072, China*
[2] *Institute for Sedimentation on River and Coastal Engineering, Tianjin 300072, China*

Abstract. The meandering river is an unstable system with the characteristic of non-linearity, which results from the instability of the flow and boundary. Focusing on the hydrodynamic nonlinearity of the bend, we use the weakly nonlinear theory and perturbation method to construct the nonlinear evolution equations of the disturbance amplitude and disturbance phase of two-dimensional flow in meandering bend. The influence of the curvature, *Re* and the disturbance wave number on the evolution of disturbance amplitude and disturbance phase are analyzed. Then, the spatial and temporal evolution of the disturbance vorticity is expounded. The research results show: that the curvature makes the flow more stable; that in the evolution of the disturbance amplitude effected by curvature, *Re* and the disturbance wave number, exist nonlinear attenuation with damping disturbances, and nonlinear explosive growth with positive disturbances; that the asymmetry distribution of the disturbance velocities increases with the curvature; that the location of the disturbance vorticity's core area changes periodically with disturbance phase, and the disturbance vorticity gradually attenuates/increases with the decrease of the disturbance phase in the evolution process of damping/positive disturbances. These results shed light on the construction of the interaction model of hydrodynamic nonlinearity and geometric nonlinearity of bed.

AMS subject classifications: 76E30, 34C60

Key words: Curvature bend, hydrodynamics, weakly nonlinearity, disturbance vorticity.

1 Introduction

Since the 1980s, scholars have kept investigating the characteristics of the stability and nonlinearity of meandering rivers. Callander [1] considered that the instability is the

*Corresponding author.
Emails:* Libin0425@tju.edu.cn (B. Li), xiaoxiaoxu_2004@163.com (H. Xu), ychbai@tju.edu.cn (Y. Bai), zqji@tju.edu.cn (Z. Ji)

cause of the river bending or braiding. In the instability analysis by Ikeda, Parker and Sawai [2], the most unstable wavelength was considered as the finite amplitude wavelength of the meandering river, which assumed the curvature ratio (the ratio of the half width to the curvature radius) is far less than 1. Parker, Sawai and Ikeda [3] analyzed the geometrical nonlinear stability of meandering river, ignoring the nonlinear dynamic terms. In the weakly nonlinear analysis of the meandering river by Seminara and Tubino [4], the geometric weakly nonlinear analysis was carried out near the resonance state, and the suppression of the nonlinear effect was revealed. Imran, Parker and Pirmez [5] pointed out that the study of Sun [6] has a fundamental defect in simulating the evolution of the meandering river because the nonlinear effect of flow dynamic is ignored. The meandering river has the instability mechanism, which refers to the instability of the flow [7]. Pittaluga, Nobile and Seminara [8] thought that the linear theory of the meandering river explains the resonance mechanism. However, the complete nonlinear theory of the meandering river has not been established yet, and the nonlinear effect has a certain influence on the flow field. Pittaluga and Seminara [9] argued that nonlinearity and instability are the important characteristics of the meandering river, while the effects of nonlinearity have been seriously ignored. Bai et al. [10–12] suggested that the nonlinear hydrodynamics theory is important to investigate the evolution of rivers under disturbances. Nelson, Pittaluga and Seminara [13] presented a nonlinear asymptotic theory of fully developed flow and bed topography subjected to unerodible bedrock layer, but they ignored the nonlinearity of the flow itself.

The previous studies mainly focused on the geometric nonlinearity of the meandering river and the bed disturbance. However, the study on the characteristics of the nonlinearity and evolution of the flow dynamics in the meandering river with different curvatures is insufficient. Different from the weakly nonlinear instability in the plane Poiseuille flow and shear layers [14, 15], in this paper, the instability and nonlinear evolution of the flow dynamics affected by the curved boundary with damping and positive disturbances are analyzed by constructing the control equation under the small flow disturbance. Under the conditions of the time mode, the Orr-Sommerfeld equation is used to analyze the stability characteristics of the hydrodynamic in the bend. And the Landau-Stuart equations are used with the weakly nonlinear theory of flow stability [16, 17]. Then the nonlinear evolution equations of the hydrodynamic of the constant curvature bend under the nonlinear effect of the flow are derived. The influences of the material composition of the river bank and the form of the bed surface are ignored. Generally, the river's curvature is constant along the bend, and the width is limited by the walls, such as in the canyon channel of Jing River in Shaanxi Province, China (Fig. 1). And in order to reduce the complexity of equations, we take the constant curvature form to investigate the stability and nonlinearity of hydrodynamic in the meandering river. The hydrodynamic study in the constant curvature bend provides the nonlinear hydrodynamic basis for further exploring the complete nonlinear relationship between river hydrodynamic and bed morphology. And in natural rivers, a high-order method is an accurate tool to study three-dimensional hydrodynamics [18].

Figure 1: The canyon meandering channel in Jing River.

2 Theoretical model

2.1 Coordinate transformations

In order to simplify the governing equations of the meandering river possibly, Parker [2, 3] and Smith [19] proposed an orthogonal curvilinear coordinate system (Fig. 2). The bend's width is proposed to be constant along the river ($2B_r$). The values of the x_0 and the y_0 are the values on the X-axis and the Y-axis of the river centerline in the Cartesian coordinate system, respectively, shown in the following figure. Then the transformation relationship between orthogonal curvilinear coordinate system and Cartesian coordinate system are as follows:

$$x = x_0 + \Delta x = x_0 - n \frac{dy_0}{ds}, \tag{2.1a}$$

$$y = y_0 + \Delta y = y_0 + n \frac{dx_0}{ds}. \tag{2.1b}$$

The radius of curvature $R(s)$:

$$R(s) = \left(\frac{dx_0}{ds} \frac{d^2 y_0}{ds^2} - \frac{dy_0}{ds} \frac{d^2 x_0}{ds^2} \right)^{-1}. \tag{2.2}$$

The relevant metric coefficients are:

$$h_s = 1 - \frac{n}{R(s)} = 1 - N, \quad h_n = 1, \quad h_z = 1. \tag{2.3}$$

2.2 Control equations of the meandering bend

The object investigated in this paper is the constant curvature bend in the two-dimensional case. Under the conditions of the orthogonal curvilinear coordinates, we
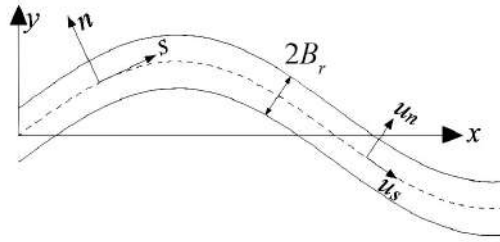
Figure 2: Orthogonal curvilinear coordinate system in the meandering river.

take B_r^*, R_m^*, and U_m^* as the half-width of the bend, the minimum curve radius and the maximum value of the base flow velocity respectively, "*" means the dimensional quantity. The scaling of the length, velocity and time are expressed by the B_r^*, U_m^*, B_r^*/U_m^*, respectively. Then we have:

$$(s^*,n^*)=B_r^*(s,n), \quad R^*=R_m^*R, \quad (u_s^*,u_n^*)=U_m^*(u_s,u_n),$$

$$p^*=\rho U_m^{*2}p, \quad t^*=\frac{B_r^*}{U_m^*}t, \quad N=\frac{B_r^*}{R_m^*}\frac{n}{R}, \quad \psi=\frac{B_r^*}{R_m^*}.$$

In the above equations, p^*, ρ, and t^* represent the pressure, the density of the flow and the time respectively. ψ, called the curvature ratio, which refers to the ratio between the half-width and the minimum curve radius, is the critical characteristic parameter of the meandering river. In the case of the constant curvature, $R=1$, so $h_s=1-\psi n$. Then we can derive the dimensionless governing equations of the meandering river with the constant curvature:

$$\frac{1}{h_s}\frac{\partial u_s}{\partial s}+\frac{\partial u_n}{\partial n}-\frac{\psi u_n}{h_s}=0, \tag{2.4a}$$

$$\frac{\partial u_s}{\partial t}+\frac{u_s}{h_s}\frac{\partial u_s}{\partial s}+u_n\frac{\partial u_s}{\partial n}-\frac{\psi u_s u_n}{h_s}=-\frac{1}{h_s}\frac{\partial p}{\partial s}+\frac{1}{Re}\overline{\Delta}u_s-\frac{\psi}{Re}\left[\frac{2}{h_s^2}\frac{\partial u_n}{\partial s}+\frac{1}{h_s}\frac{\partial u_s}{\partial n}+\frac{\psi u_s}{h_s^2}\right], \tag{2.4b}$$

$$\frac{\partial u_n}{\partial t}+\frac{u_s}{h_s}\frac{\partial u_n}{\partial s}+u_n\frac{\partial u_n}{\partial n}-\frac{\psi u_s^2}{h_s}=-\frac{\partial p}{\partial n}+\frac{1}{Re}\overline{\Delta}u_n+\frac{\psi}{Re}\left[\frac{2}{h_s^2}\frac{\partial u_s}{\partial s}-\frac{1}{h_s}\frac{\partial u_n}{\partial n}-\frac{\psi u_n}{h_s^2}\right]. \tag{2.4c}$$

In the above equations: $Re(=\frac{B_r^* U_m^*}{\nu})$ is the Reynolds number, ν is the kinematic viscosity, $\overline{\Delta}=\frac{1}{h_s^2}\frac{\partial^2}{\partial s^2}+\frac{\partial^2}{\partial n^2}$.

2.3 Perturbation analysis

The study of Zachmann and Lagasse [20] shows that the value of ψ in natural rivers is mainly distributed at $0.05\sim 0.20$. Therefore, in our study, ψ is regarded as a small parameter; Eqs. (2.4a)-(2.4c) are solved with the perturbation method; and the velocity
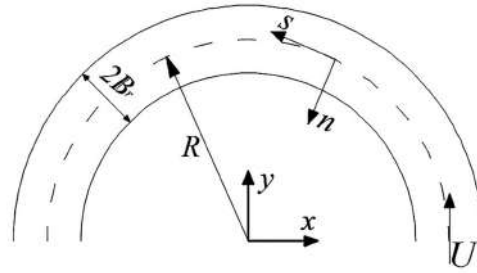
Figure 3: Sketch illustrating the constant curve river.

and pressure are divided into three parts:

$$
\begin{bmatrix} u_s \\ u_n \\ p \end{bmatrix} = \begin{bmatrix} u_{s_{\psi 0}} \\ u_{n_{\psi 0}} \\ p_{\psi 0} \end{bmatrix} + \sum_{i=1}^{\infty} \psi^i \begin{bmatrix} u_{s_{\psi_i}} \\ u_{n_{\psi_i}} \\ p_{\psi_i} \end{bmatrix} + \sum_{i=1}^{\infty} \varepsilon^i \begin{bmatrix} u_{s_i} \\ u_{n_i} \\ p_i \end{bmatrix}. \tag{2.5}
$$

At the right of the above equation, the first part is the base flow of the open channel; the second part is the curvature correction terms, which relate to ψ; the third part is the flow disturbance terms, which consider the nonlinear effect arising from the flow disturbance in the meandering river, and ε is an any small quantity. In the analysis of the base flow terms and the curvature correction terms, because ψ is far less than 1, thus the influence caused by weak curvature can only consider the effect of the first-order of ψ.

Considering the base flow terms of the open channel in Eq. (2.5), we set $\psi = 0$, $u_{n_{\psi 0}} = 0$, $\partial/\partial s = \partial/\partial t = 0$, and the corresponding boundary conditions as $u_{n_{\psi 0}} = u_{s_{\psi 0}} = 0$ $(n = \pm 1)$. And then the solutions of the velocity and pressure are as follow:

$$
u_{n_{\psi 0}} = 0, \quad u_{s_{\psi 0}} = 1 - n^2, \quad p_{\psi 0} = 0. \tag{2.6}
$$

The curvature correction terms, $u_{s_{\psi 1}}$, $u_{n_{\psi 1}}$, $p_{\psi 1}$ in the constant curvature bend are:

$$
u_{n_{\psi 1}} = 0, \quad u_{s_{\psi 1}} = -\frac{1}{3}(n - n^3), \quad p_{\psi 1} = -n - \frac{1}{5}n^5 + \frac{2}{3}n^3. \tag{2.7}
$$

The base flow terms and the first-order curvature correction terms are combined as the base flow of the constant curvature bend. And then, the base flow terms and the flow disturbance terms are brought into the control equations of the constant curvature bend thus we have:

$$
\begin{bmatrix} u_s \\ u_n \\ p \end{bmatrix} = \begin{bmatrix} 1 - n^2 - \dfrac{\psi}{3}(n - n^3) \\ 0 \\ \psi\left(-n - \dfrac{1}{5}n^5 + \dfrac{2}{3}n^3\right) \end{bmatrix} + \sum_{i=1}^{\infty} \varepsilon^i \begin{bmatrix} u_{s_i} \\ u_{n_i} \\ p_i \end{bmatrix} = \begin{bmatrix} \overline{u}_s \\ \overline{u}_n \\ \overline{p} \end{bmatrix} + \sum_{i=1}^{\infty} \varepsilon^i \begin{bmatrix} u_{s_i} \\ u_{n_i} \\ p_i \end{bmatrix}. \tag{2.8}
$$

In Eq. (2.8), $\overline{u}_s$, $\overline{u}_n$, and $\overline{p}$ are the streamwise velocity, cross-section velocity, and pressure of the base flow in the constant curvature bend, respectively. We take Eq. (2.8) to Eqs. (2.4a)-(2.4c), and then the perturbation control equations of any order can be obtained

$$\sum_{i=1}^{\infty}\left\{\frac{1}{h_s}\frac{\partial u_{s_i}}{\partial s}+\frac{\partial u_{n_i}}{\partial n}-\frac{\psi u_{n_i}}{h_s}\right\}=0, \tag{2.9a}$$

$$\sum_{i=1}^{\infty}\left\{\frac{\partial u_{s_i}}{\partial t}+Lu_{s_i}+u_{n_i}\frac{\partial\overline{u}_s}{\partial n}+\frac{1}{h_s}\frac{\partial p_i}{\partial s}-\frac{\psi\overline{u}_s u_{n_i}}{h_s}+\frac{\psi}{Re}\left[\frac{2}{h_s^2}\frac{\partial u_{n_i}}{\partial s}+\frac{1}{h_s}\frac{u_{s_i}}{\partial n}+\frac{\psi u_{s_i}}{h_s^2}\right]\right\}\varepsilon^i$$

$$=-\varepsilon\sum_{i=1}^{\infty}\sum_{j,k\leq1}^{j+k=i+1}\left(\frac{1}{h_s}u_{s_j}\frac{\partial u_{s_k}}{\partial n}+u_{n_j}\frac{\partial u_{s_k}}{\partial n}-\frac{\psi u_{s_j}u_{n_k}}{h_s}\right)\varepsilon^i, \tag{2.9b}$$

$$\sum_{i=1}^{\infty}\left\{\frac{\partial u_{n_i}}{\partial t}+Lu_{n_i}+\frac{\partial p_i}{\partial n}+2\frac{\psi\overline{u}_s u_{s_i}}{h_s}+\frac{\psi}{Re}\left[\frac{-2}{h_s^2}\frac{\partial u_{s_i}}{\partial s}+\frac{1}{h_s}\frac{u_{n_i}}{\partial n}+\frac{\psi u_{n_i}}{h_s^2}\right]\right\}\varepsilon^i$$

$$=-\varepsilon\sum_{i=1}^{\infty}\sum_{j,k\leq1}^{j+k=i+1}\left(\frac{1}{h_s}u_{s_j}\frac{\partial u_{n_k}}{\partial n}+u_{n_j}\frac{\partial u_{n_k}}{\partial n}+\frac{\psi u_{s_j}u_{s_k}}{h_s}\right)\varepsilon^i. \tag{2.9c}$$

In the above equations,

$$L=\frac{\overline{u}_s}{h_s}\frac{\partial}{\partial s}-\frac{1}{Re}\left(\frac{1}{h_s^2}\frac{\partial^2}{\partial s^2}+\frac{\partial^2}{\partial n^2}\right)$$

and i means the order ($i=1,2,\cdots$).

2.4 Linear stability analysis

In the linear instability analysis of shear flow, Wu [21] introduced a small amplitude perturbation based on the base flow and obtained the solution form by separating variables based on the approximate local parallel flow. In this paper, as $\overline{u}_s$, $\overline{u}_n$, and $\overline{p}$ in Eq. (2.8) are merely the function of n, and the flow disturbance is considered a small amplitude quantity. Therefore, the first-order disturbance quantity of u_{s_1}, u_{n_1}, p_1 can be written as:

$$\begin{bmatrix}u_{s_1}\\u_{n_1}\\p_1\end{bmatrix}=\begin{bmatrix}\hat{u}_{s_1(n)}\\\hat{u}_{n_1(n)}\\\hat{p}_{1(n)}\end{bmatrix}\exp[i(\alpha s-\omega t)]+c.c. \tag{2.10}$$

In the above equations, $\hat{u}_{s_1(n)}$, $\hat{u}_{n_1(n)}$, $\hat{p}_{1(n)}$ are the shape functions about n; α is the disturbance wave number; ω is the disturbance frequency; and $c.c$ is the conjugate complex number. We take Eq. (2.10) into Eqs. (2.9a)-(2.9c) and then get the governing equations of the first-order disturbance. Our goal is to investigate the flow's instability and nonlinear evolution process in the constant curvature bend under the time mode. Therefore, the disturbance frequency can be written as $\omega=\omega_r+i\omega_i$. The imaginary part of the disturbance frequency (ω_i) is related to the increase or decrease of the disturbance. Then the

disturbance amplitude and disturbance phase can be written as $a=\exp(\omega_i t)$ and $\theta=-\omega_r t$, respectively, and both of them satisfy the relation as follows:

$$F(\alpha,\omega,Re,\psi)=0. \tag{2.11}$$

The Eq. (2.11) is the Orr-Sommerfeld equation for hydrodynamic characteristics of the meandering channel with the constant curvature. Then under the influence of curvature and the corresponding variation of the disturbance wave number and Reynolds number, the neutral curve distribution can be obtained. The central difference method and Muller method are used to solve Eq. (2.11). It can be calculated with the change of the ω_r, ω_i under specific Re and α. When $\omega_i=0$, it is called the neutral state.

2.5 Nonlinear evolution equations under time mode

Wu [21] pointed out that the weakly nonlinear theory is closely related to the development of shear flow at high Reynolds number. Due to the influence of nonlinearity, the evolution process of the flow hydrodynamic can be expressed by the disturbance amplitude function. Moreover, higher harmonic terms are generated due to the nonlinear interaction. In the nonlinear evolution of the hydrodynamics process in the constant curvature bend, we use the classical weakly nonlinear theory of the Landau-Stuart equation [16] under the time mode. Because of the effect of nonlinearity, the evolution of the disturbance amplitude and disturbance phase can be expressed as follows:

$$\frac{da}{dt}=\omega_i a+\sum_{m=1}^{\infty} A_m a^m = A, \quad \frac{d\theta}{dt}=-\omega_r+\sum_{m=1}^{\infty} B_m a^m = B. \tag{2.12}$$

And according to the chain rule, we have:

$$\frac{\partial u_i}{\partial t}=\frac{\partial u_i}{\partial a}\left(\omega_i a+\sum_{m=1}^{\infty} A_m a^m\right)+\frac{\partial u_i}{\partial \theta}\left(-\omega_r+\sum_{m=1}^{\infty} B_m a^m\right). \tag{2.13}$$

In Eq. (2.12), $A_0=\omega_i a$, $B_0=-\omega_r$, $a=e^{\omega_i t}$, $\theta=-\omega_r t$. A_m and B_m, $(m=1,2,\cdots)$ are the Landau coefficients. In Eq. (2.13), u_i, $(i=1,2,\cdots)$ is the disturbance velocity component at any order. If we take Eq. (2.13) back to Eqs. (2.9a)-(2.9c), then the weakly nonlinear evolution equations of the constant curvature bend can be obtained at any order. Seminara [9] pointed out that the analysis of the meandering river needs complete nonlinear governing equations for simulation, and the effect of the sidewall boundary layer cannot be ignored. The corresponding boundary conditions of the flow disturbance on the sidewall in our study are:

$$u_{n_i}=u_{s_i}=0, \quad (n=\pm 1, \quad i=1,2,\cdots). \tag{2.14}$$

Then the perturbed control equations of the first order to the fifth order under the weakly nonlinear evolution of the constant curvature bend under the time mode are obtained. The perturbed control equations are solved by the central difference method.

3 Results

3.1 Model validation and neutral curve of stability theory

The critical Reynolds number (Re_{cr}) and neutral curve calculated when $\psi = 0$ are compared with the experiment results of the plane Poiseuille flow made by Nishioka [22]. And we take the results of Re from Orszag [23] as the critical Reynolds number ($Re_{cr} = 5772.22$ and $\alpha = 1.02059$). And the results in our model, $Re_{cr} = 5772.2222$ and $\alpha = 1.02059$, are consistent with the results of Nishioka and Orzag (Fig. 4(a)). In terms of the nonlinear evolution of the disturbance velocity, we compare our results with that of Zhou and You [14] in the evolution of u_1, u_{20} and u_{22} under the conditions of $\psi = 0$, $Re = 10000$, $\alpha = 1.096$, $\omega_r = 0.270284$, $\omega_i = 0.000088$ (Fig. 4(b)), which are consistent well.

The black dots in Fig. 5 and Fig. 6 show the distribution of Re_{cr} under different ψ. $c_r (= \omega_r / \alpha)$ is the real part of the disturbance wave velocity (Fig. 6). The results show that with the increase of ψ, the neutral curve moves toward the direction of the increasing Re. The region outside the neutral curve is stable while the region inside the neutral curve is unstable, which means with the increase of ψ, the area of the unstable region reduces, the flow in the bend tends to be more stable and loses the stability at the higher Reynolds number, which is consistent to the result of Bai et al. [24].

Except at Re_{cr}, there are two different neutral points at the neutral curve for the same Re at the upper and lower branches, respectively. And with the increase of ψ, α, and c_r get closer to the lower branch. With the limit of the weak curvature ratio, ψ increases from 0 to 0.20, Re_{cr} increases exponentially, while α and c_r show a downward trend monotonously (Fig. 7). It is because the curved boundary impacts on the flow, which relates to the interaction among ψ and α, c_r, as well as Re in Eq. (2.11). Besides, the results also reveal that the river boundary is often curved in nature.
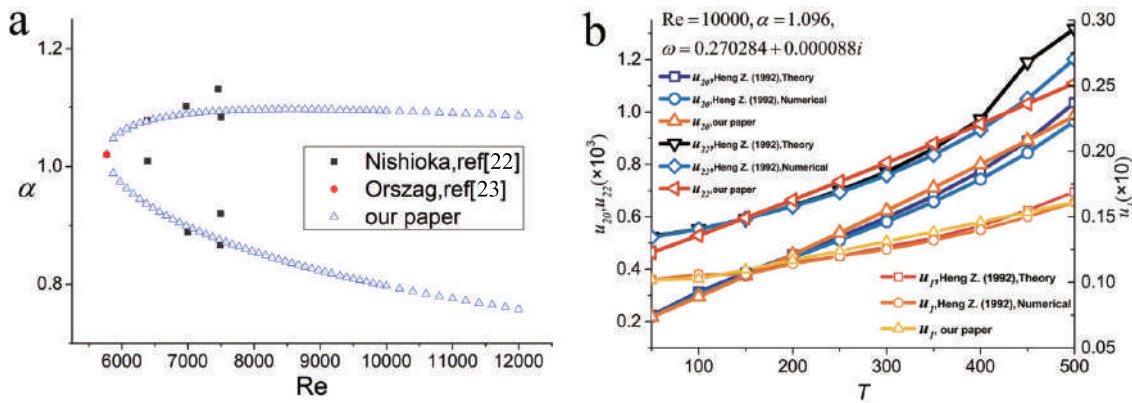

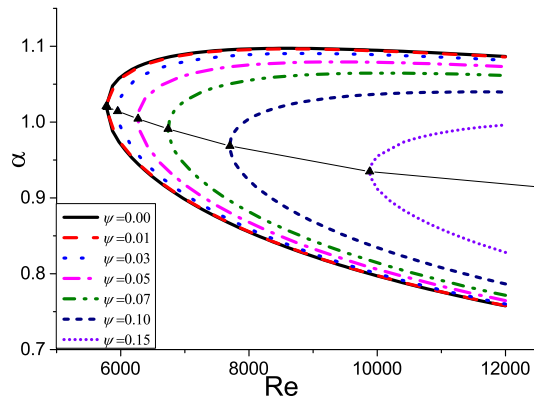Figure 4: Verification of neutral curve $Re - a$ (a) and the disturbance velocity (b).

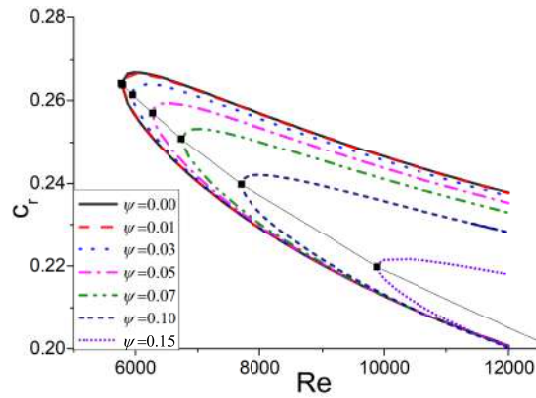Figure 5: Effect of curvature on neutral curve of $Re-\alpha$.

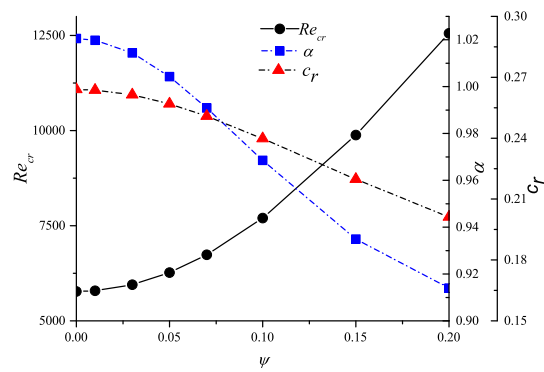Figure 6: Effect of curvature on neutral curve of $Re-c_r$.

Figure 7: Stability characteristics under different curvature ratio.

4 Discussion

4.1 Evolution characteristics of the disturbance amplitude and disturbance phase

After obtaining Landau coefficients of A and B by using the solvable condition, the initial disturbance amplitude (a_0) is set to be 0.01 for analysis. The values of α and c_r near the neutral curve (see Supplement A) are taken to analyze the influence of different ψ on the evolution of the disturbance amplitude (a) and disturbance phase (θ) near the neutral curve with damping and positive disturbances, respectively. In the following analysis, the imaginary part of the disturbance wave velocity is taken as c_i ($=\omega_i/\alpha$) $= 0.005$ and -0.005, respectively. In a high-Reynolds number shear layer, the nonlinear evolution of a pair of initially linear oblique waves can induce the explosive growth by nonlinear effects [15]. So we aim to reveal the evolution characteristics of the positive and damping disturbances under the weak nonlinear effect.

When Re keeps the same, with the increase of ψ, the attenuation rate of a increases when $c_i = -0.005$ (Fig. 8). However, when time increases to a certain value, the value of the disturbance amplitude decreases to 0, the initial disturbance will disappear after a certain period under negative c_i. This effect can be called nonlinear attenuation. While $c_i = 0.005$, the disturbance amplitude increases with time, and explosively grows when time reaches a critical value. And we found that the larger ψ is, the larger a is. However, when time reaches another critical value, the magnitude of a under $\psi = 0$ is larger than that of $\psi = 0.05 \sim 0.10$, which means that the existence of ψ will reduce the increase rate of a under positive c_i. θ presents a monotonic decreasing trend with time when c_i is negative. When c_i is positive and the time value is larger than critical value, with the nonlinear effect, θ is explosively increased when $\psi \leq 0.05$ and explosively decreases when $\psi \geq 0.07$.

Figure 8: Evolution process of the disturbance amplitude and disturbance phase under different ψ (left: the disturbance amplitude; right: the disturbance phase, $Re = 10000$).
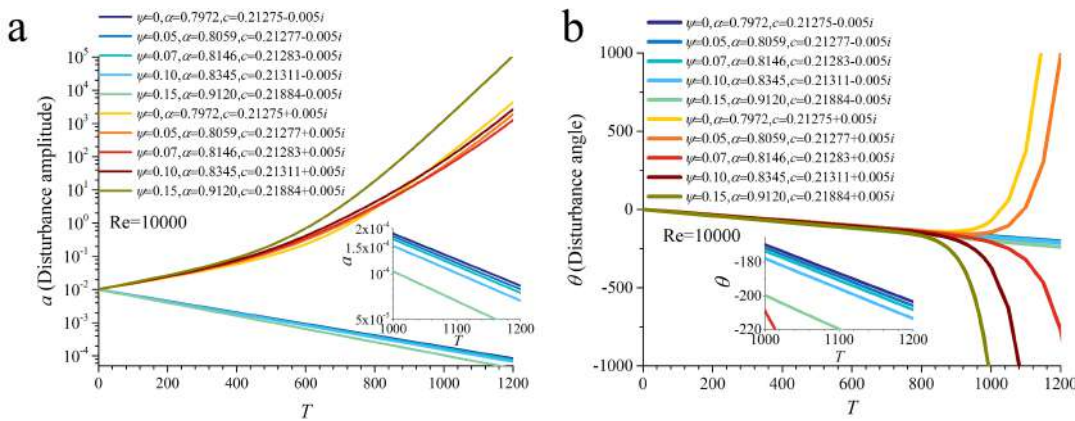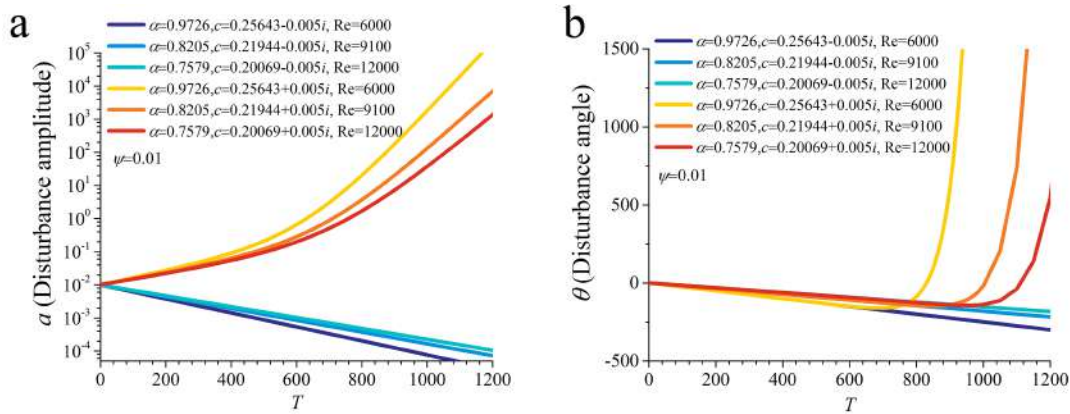
Figure 9: Evolution process of the disturbance amplitude and disturbance phase under different Re (left: the disturbance amplitude; right: the disturbance phase, $\psi = 0.01$).
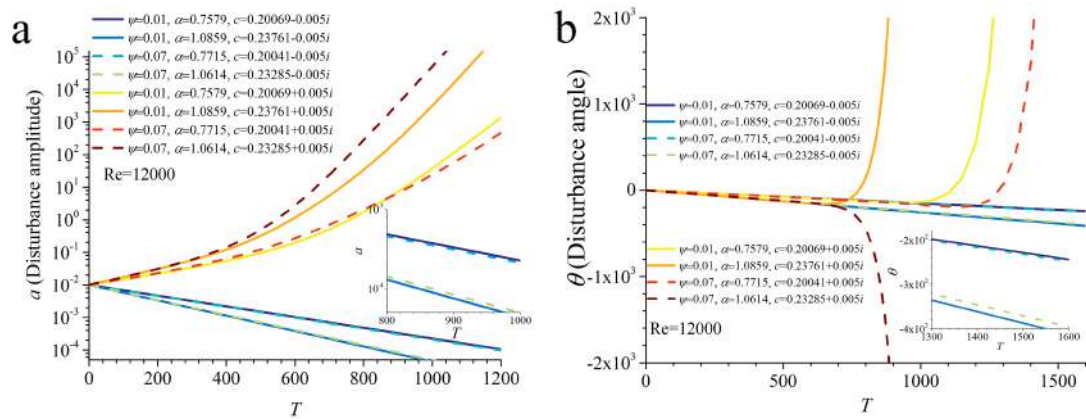

Figure 10: Evolution process of the disturbance amplitude and disturbance phase under different α (left: the disturbance amplitude; right: the disturbance phase, $Re = 12000$)

When $\psi \leq 0.05$, the lower ψ is, the larger θ is, while when $\psi \geq 0.07$, the result is reversed, which is related to the *Landau* coefficient.

We take $\psi = 0.01$, $Re = 6000$ to 12000 to analyze the evolution characteristics of a and θ with Re. When $c_i = -0.005$, both a and θ decrease with Re, and the larger Re is, the larger the decreasing rate of a and θ is. While c_i is positive, the larger Re is, the lower value of a is. However, θ decreases with the increase of time. When time reaches critical values, θ is in explosive growth and the critical time value increases with Re.

There are two different values of the disturbance wave number or disturbance wave velocity at the neutral curve, except for Re_{cr}. In order to investigate the influence of the disturbance wave number on the disturbance amplitude and disturbance phase, we

take $\psi = 0.01$ and 0.07, $Re = 12000$, $\alpha = 1.0859$ and 1.0614 at the upper branch, and $\alpha = 0.7579$ and 0.7715 at the lower branch and then analyze respectively, as shown in Fig. 10. With the same Re, time, and c_i, the larger α is, the larger the absolute value of a is. And when $c_i = 0.005$, a increases faster with high values of ψ, but when time reaches a certain value, a increases slower under the effect of curvature. In terms of θ, the larger α is, the larger the magnitude of θ is. When c_i is positive, the critical time value of the explosive growth/decrease point is smaller when α is larger.

4.2   Distribution of the disturbance velocity

The real part and the imaginary part of the components of the disturbance velocity can be written as:

$$u_{sr} = Real\left(\sum_{i=1}^{5}\varepsilon^i u_{s_i}\right), \qquad\qquad u_{si} = Img\left(\sum_{i=1}^{5}\varepsilon^i u_{s_i}\right), \qquad (4.1a)$$

$$u_{nr} = Real\left(\sum_{i=1}^{5}\varepsilon^i u_{n_i}\right), \qquad\qquad u_{ni} = Img\left(\sum_{i=1}^{5}\varepsilon^i u_{n_i}\right). \qquad (4.1b)$$

In Eq. (4.1), $Real$ and Img mean the real part and imaginary part, respectively, and ε is any small quantity. We take a (disturbance amplitude) to replace ε, neglect the effect of the correction of the base flow and then analyze the distribution of the disturbance velocity.

4.2.1   Influence of the disturbance phase on the disturbance velocity

We aim to investigate the evolution characteristics of the disturbance velocity under different θ ranging from -4π to -6π. And we take $\psi = 0.10$, $s = 0$, $k = \theta$, $a_0 = 0.01$.

The distribution of the streamwise disturbance velocity (u_{sr}) in Figs. 11(a) and (c) presents the sigmoid shape, which means that the maximum value is close to both sides. Nevertheless, there is a turning point near the region of $n = -1$. When θ ranges from -4π to -6π, u_{sr} near $n = 1$ decreases to $\theta = -5\pi$ and then increases in other periods. As u_{sr} approaches to $n = -1$, the turning point increase to the maximum till $\theta = -4\pi - 2\pi/3$. The shape function of u_{sr} is the same when c_i is positive and negative.

The distribution of the cross-section disturbance velocity (u_{nr}) presents parabolic shape. The location of the maximum absolute value of the disturbance velocity ranges from $n = 0.2$ to 0.4, which is influenced by ψ. And this position changes with θ, which moves to $n = 1$ when θ ranges from $-4\pi - \pi/3$ to -5π. In some certain values of θ ($= -4\pi$), there exists the sigmoid shape of u_{nr}, and the magnitude of u_{nr} near $n = 1$ is larger than that near $n = -1$.

4.2.2   Influence of the curvature ratio on the shape function of the disturbance velocity

For investigating the effect of ψ on the shape of the disturbance velocity, we take $\psi = 0.03 \sim 0.15$, $Re = 10000$, $s = 0$, $c_i = -0.005$ and 0.005. α and c_r from the neutral curve (Supplement A) and $\theta = -4\pi$ to -5π.
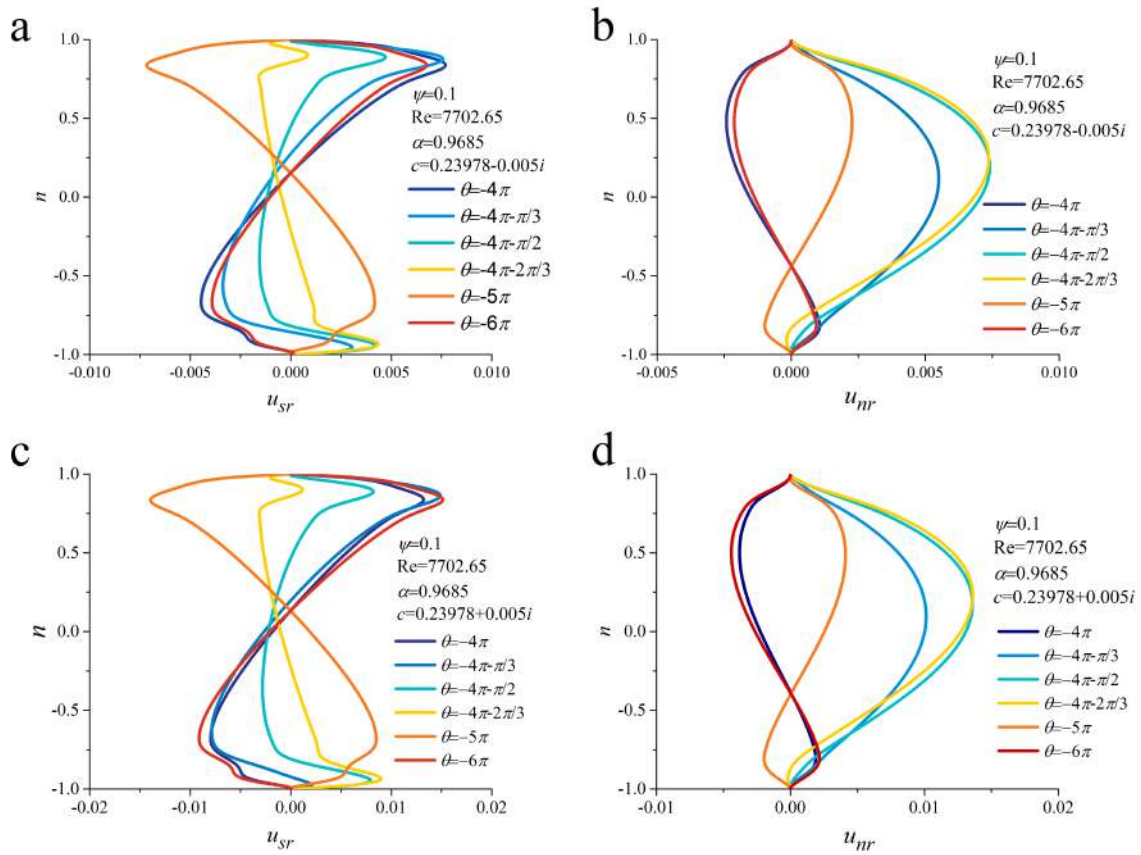
Figure 11: The distribution of the disturbance velocity under different θ.

The streamwise disturbance velocities (u_{sr} and u_{si}) at the cross-section of $s=0$ present the sigmoid shape under different ψ. When ψ is large, such as $\psi=0.15$, the distribution of u_{sr} near $n=-1$ shows a velocity turning point. Below the point, the direction of u_{sr} keeps the same with u_{sr} near $n=1$. Apart from this turning point, an extremum value near $n=-1$ occurs corresponds to the extremum value of velocity near $n=1$. With the increase of ψ, the symmetry of u_{sr} and u_{si} decreases gradually. The extremum value of u_{sr} near $n=-1$ decreases with the increase of ψ, and when $\psi=0.15$ and $\theta=-4\pi$, the magnitude of maximum value of u_{sr} near $n=-1$ is only half of that near $n=1$.

The transverse disturbance velocities (u_{nr} and u_{ni}) at the cross-section of $s=0$ present the parabolic shape. But when ψ is larger ($\psi=0.10, 0.15$), $\theta=-4\pi$ and -5π, the distribution of u_{nr} presents the sigmoid shape, and the magnitude of u_{nr} near $n<0$ is lower than that on the other side. This phenomenon also exists in the distribution of u_{ni}. These results show that the distribution of u_{nr} and u_{ni} will move toward the direction of $n=1$ with the increase of ψ, and the symmetry of the distribution of u_{nr}/u_{ni} also transfers
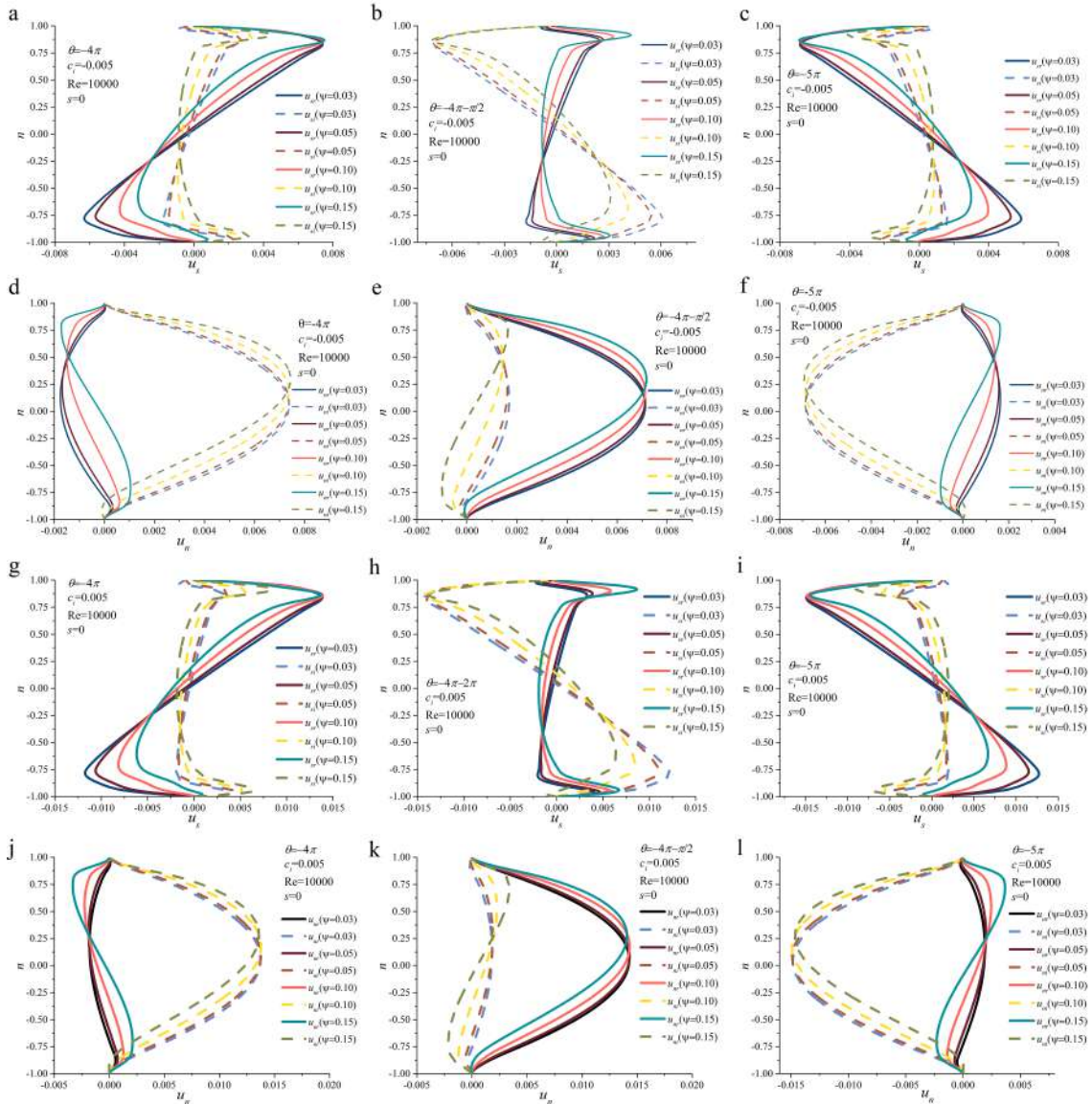
Figure 12: The distribution of the disturbance velocity under different ψ ($Re\!=\!10000$).

to asymmetry gradually. The shape function of the disturbance velocity keeps the same when $c_i = -0.005$ and 0.005.

4.2.3 Influence of the Reynolds number on the disturbance velocity

In order to investigate the effect of Re on the disturbance velocity under different θ, we take $\psi = 0.10$, $Re = 9000, 10000, 12000$, respectively, $c_i = -0.005$ and 0.005, $s = 0$, α and c_r
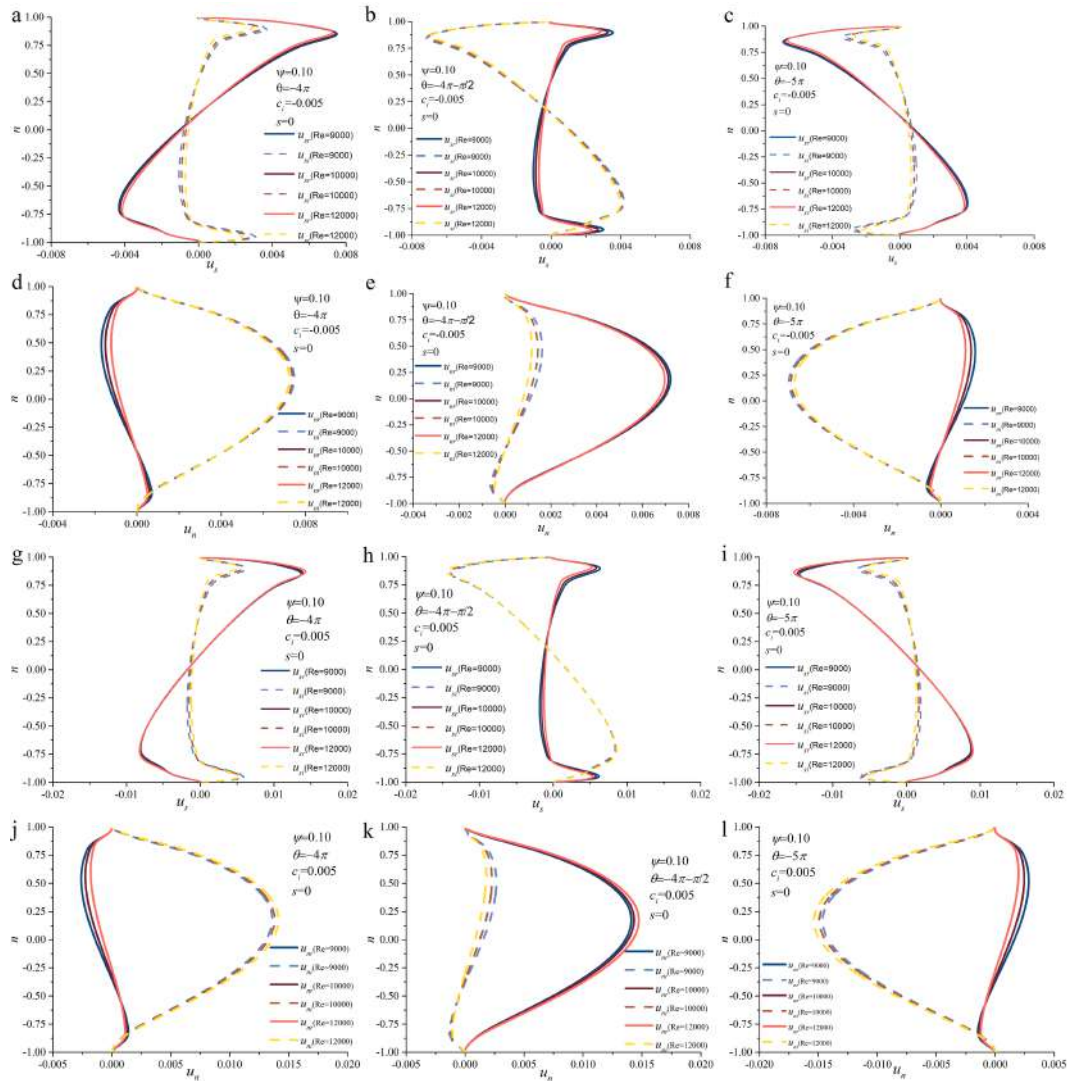
Figure 13: The distribution of the disturbance velocity under different Re.

from the neutral curve (Supplement A), and θ ranging from -4π to -5π.

In Fig. 13, the characteristics of both the disturbance velocity in streamwise and transverse are as follow. Firstly, at the same θ, with the increase of Re, the extreme values of u_{sr} and u_{si} decrease when $c_i = -0.005$ and $\theta = -4\pi, -5\pi$, while when $c_i = 0.005$, the condition is reversed. The changes of Re do not influence the shape function of the disturbance velocity. Secondly, with the increase of Re, the extreme values of u_{nr} and u_{ni} decrease when $c_i = -0.005$ and $\theta = -4\pi - \pi/2$, while when $c_i = 0.005$, the condition is reversed. From the analysis above, we can conclude that with the increase of Re, the extreme value of

the disturbance velocity decreases when c_i is negative and increases when c_i is positive. However, the changes of Re have not influenced the shape function of the disturbance velocity.

4.3　Distribution characteristics of the disturbance vorticity

For the investigation of the distribution of the velocity and vorticity in the whole constant curvature bend, we take $\psi = 0.10$, $Re = 10000$, $c_i = -0.005$ and 0.005, α and c_r from the neutral curve (Supplement A) and θ ranging from -4π to -5π.

The distribution of the disturbance vorticity ($\Omega = \frac{1}{h_s}\frac{\partial u_n}{\partial s} - \frac{\partial u_s}{\partial n} + \frac{u_s}{h_s R}$) in the whole con-
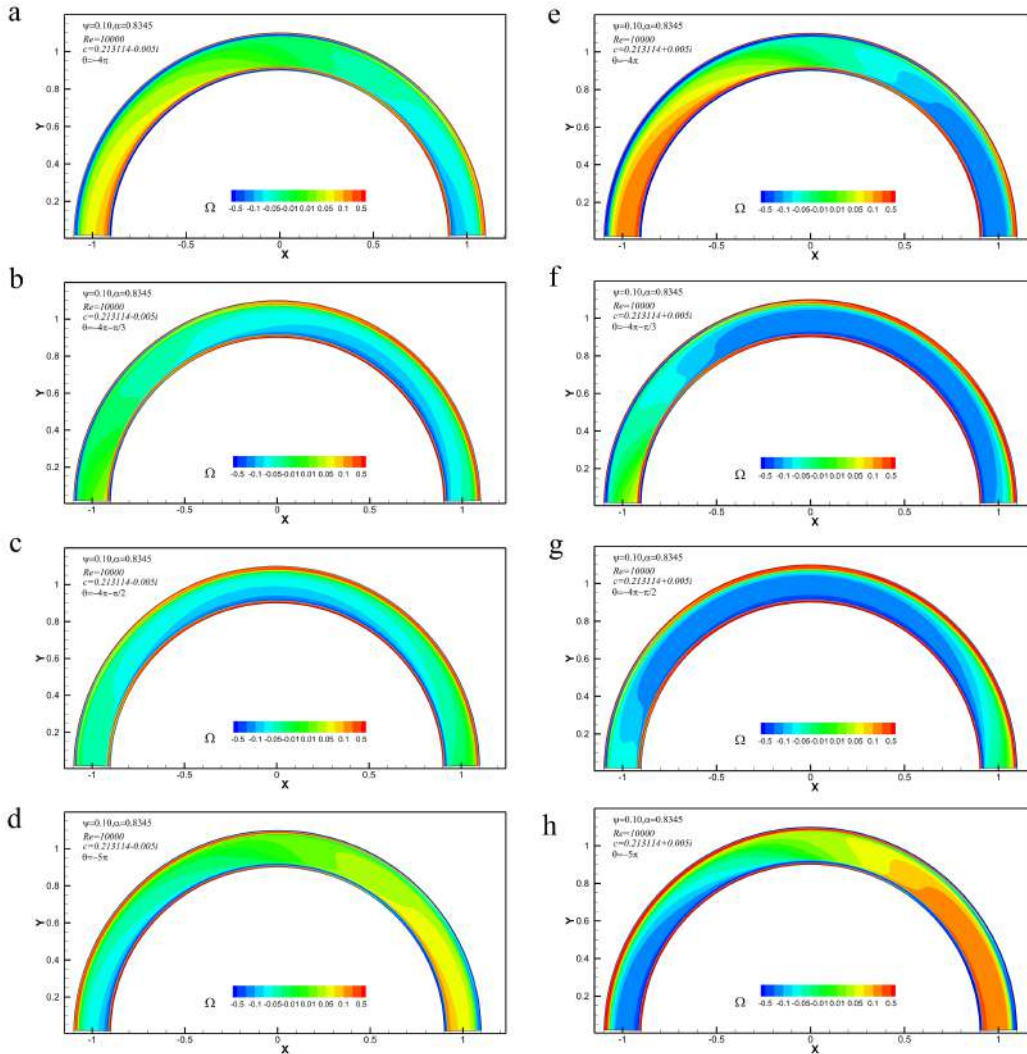

Figure 14: The distribution of the disturbance vorticity under different θ in the whole constant curvature bend.
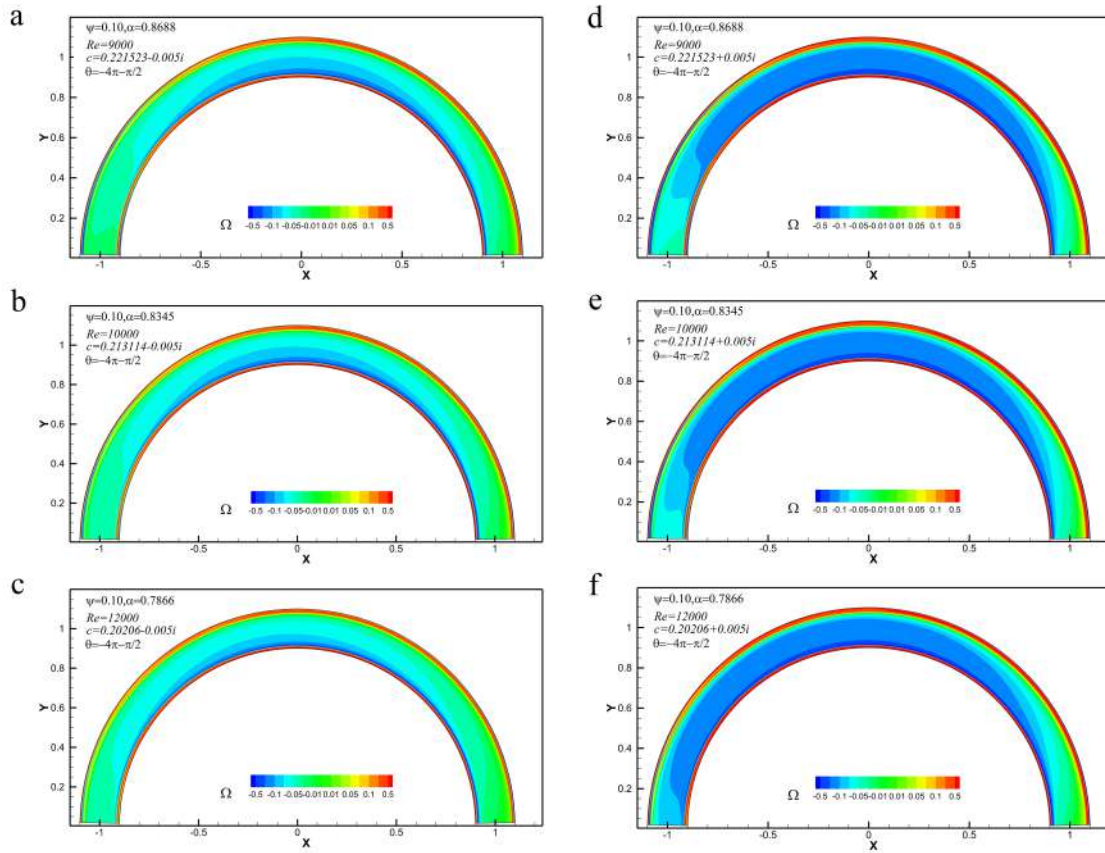
Figure 15: The distribution of the disturbance vorticity under different Re in the whole constant curvature bend.

stant curvature bend is characterized that Ω is negative (the clockwise is positive) at the entrance. However, it is positive at the end of the bend when $\theta = -4\pi$ (Fig. 14). With the decrease of θ (increasing in the negative direction), the negative Ω at the entrance begins to migrate downstream. When θ decreases to -5π, Ω is positive at the entrance of the bend, and negative at the end of the bend. Therefore, in the whole period of θ, the negative Ω begins to occupy the center of the bend and gradually moves downstream. The positive disturbance vorticity begins to develop, moving downstream and occupying the whole bend in the next half period. And the core area of Ω changes with θ. When c_i is negative, the core area's intensity of Ω decreases gradually with θ, while it increases with θ when c_i is positive.

In order to investigate the influence of Re on the distribution of the disturbance vorticity in the whole constant curvature bend, we take $\psi = 0.10$, $Re = 9000, 10000, 12000$, $c_i = -0.005$ and 0.005, $\theta = -4\pi - \pi/2$, α and c_r from the neutral curve (Supplement A). The results are shown in Fig. 15. Through the distribution of Ω at different Re, it can be seen that near the center area of bend apex, with the increase of Re, the magnitude value
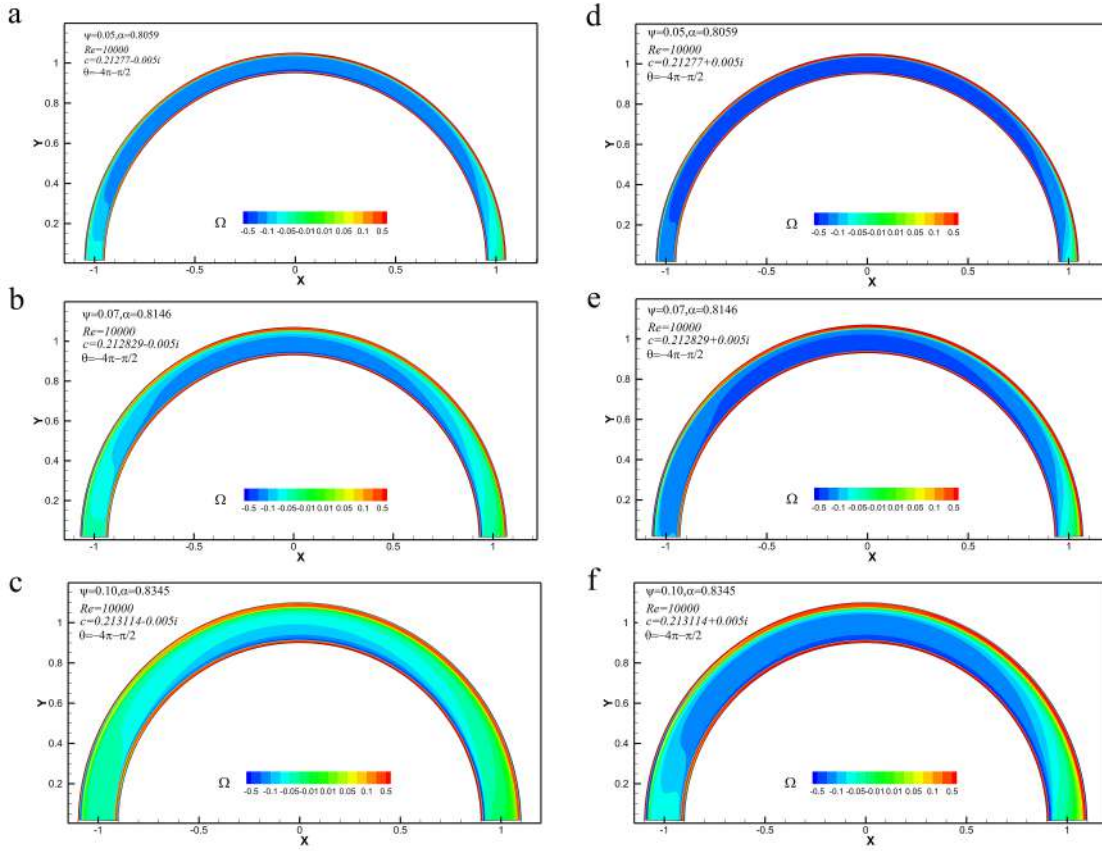
Figure 16: The distribution of the disturbance vorticity under different ψ in the whole constant curvature bend.

of Ω decreases as $c_i = -0.005$ and increases as $c_i = 0.005$. The higher magnitude value of Ω is located near both sides. However, the variation of Re does not affect the spatial and temporal evolution trend of the disturbance vorticity distribution but changes the magnitude of the disturbance vorticity.

Then, we investigate the influence of ψ on the disturbance vorticity's distribution in the whole constant curvature bend, we take $\psi = 0.05, 0.07, 0.10$, respectively, $Re = 10000$, $c_i = -0.005$ and 0.005, $\theta = -4\pi - \pi/2$, α and c_r from the neutral curve (Supplement A) (Fig. 16). With the increase of ψ from 0.05 to 0.10, the strength of Ω around the bend center area decreases gradually, and the negative value of Ω approaches the concave band ($n = 1$) gradually. From the whole distribution of Ω, the existence of ψ does not cause any phase lag. The locations of the maximum value of Ω are near both side walls. Ω rapidly decays when it gets away from the side wall. Combined with Fig. 11, it can be seen that with the increase of ψ, Ω near the side of $n = 1$ gradually strengthens, while it weakens on the side of $n = -1$.

5 Conclusions

The characteristics of flow stability and nonlinear evolution under the influence of ψ (curvature ratio), Re (Reynolds number) and θ (disturbance phase) in the constant curvature bend under damping/poistive disturbances are studied in our paper. The conclusions are as follows:

1. In the constant curvature bend, with the increase of ψ, the neutral curve moves in the direction of the increasing Re, and the corresponding Re_{cr} (the critical Reynolds number) also increases, making the bend tend to be stable. Under the small values of ψ, α (the disturbance wave number) and c_r (the real part of the disturbance wave velocity) corresponding to Re_{cr} monotonically decrease with the increase of ψ.

2. The nonlinear evolution characteristics of a (disturbance amplitude) and θ in time mode are as follows: when c_i (the imaginary part of the disturabnce wave velocity) is negative, the attenuation rates of a and θ are larger with ψ. The attenuation rates of a and θ (increases in negative direction) are lower with the increase of Re. When α is larger, the attenuation rate of a and θ is faster. When c_i is positive and time reaches the critical value under the nonlinear effect, a grows explosively, and the increasing rate is larger when α, ψ, and Re is larger. Moreover, the explosive growth exists in the evolution of θ, and the critical time value increases with the increase of Re and decreases of α and ψ, while $\psi \geq 0.07$, the explosive growth changed to explosive decrease.

3. The distribution of the streamwise disturbance velocity shows the sigmoid shape, while the parabola style in the transverse disturbance velocity, both of them changing periodically with θ. The symmetry of the disturbance velocities in both the streamwise and transverse directions decreases gradually with ψ, and shifts toward the convex bank ($n=1$). With the increase of Re, the magnitudes of the disturbance velocity decrease/increase both in the streamwise and transverse direction when c_i is negative/positive. The values of c_i and Re rarely influence on the shape function of the disturbance velocity.

4. The characteristics of the disturbance vorticity (Ω)'s evolution in the constant curvature bend are as follows: (1) In the half period of $\theta(-4\pi \sim -5\pi)$, Ω moves from the entrance to the exit gradually; in the other half period, the direction of disturbance vortex turns, and the location of the disturbance vortex core changes with θ. (2) Around the center bend, Ω decays gradually and shifts to both sides with Re, but it would not have much influence on the spatial-temporal evolution of Ω. (3) With the increase of ψ, Ω around the center will gradually decays, and moves to the convex bank. And Ω increases near the side of the convex bank ($n=1$) and decays near the side of the concave bank ($n=-1$) when ψ is larger.

Acknowledgements

References

[1] CALLANDER, *Instability and river channels*, J. Fluid Mech., 3 (1969), pp. 465–480.

[2] S. IKEDA, G. PARKER, AND K. SAWAI, *Bend theory of river meanders. Part 1. Linear development*, J. Fluid Mech., 122 (1981), pp. 363–377.

[3] G. PARKER, K. SAWAI AND S. IKEDA, *Bend theory of river meanders. Part 2. Nonlinear deformation of finite-amplitude bends*, J. Fluid Mech., 115 (1982), pp. 303–314.

[4] G. SEMINARA AND M. TUBINO, *Weakly nonlinear theory of regular meanders*, J. Fluid Mech., 244 (1992), pp.257–288.

[5] J. IMRAN, G. PARKER AND C. PIRMEZ, *A nonlinear model of flow in meandering submarine and subaerial channels*, J. Fluid Mech., 400 (1999), pp. 295–331.

[6] T. SUN, *A simulation model for meandering rivers*, Water Resour. Res., 32 (1996), pp. 2937–2954.

[7] G. SEMINARA, *Meanders*, J. Fluid Mech., 554 (2006), pp. 271–297.

[8] M. B. PITTALUGA, G. NOBILE AND G. SEMINARA, *A nonlinear model for river meandering*, Water Resour. Res., 45 (2009), pp. 1–22.

[9] M. B. PITTALUGA, AND G. SEMIARA, *Nonlinearity and unsteadiness in river meandering: a review of progress in theory and modelling*, Earth Surf. Processes Landforms, 36 (2011), pp. 20–38.

[10] Y. C. BAI AND Z. Y. WANG, *Theory and application of nonlinear river dynamics*, Int. J. Sediment Res., 29 (2014), pp. 285–303.

[11] H. J. XU AND Y. C. BAI, *Theoretical analyses on hydrodynamic instability in narrow deep river with variable curvature*, J. Appl. Math. Mech., 36 (2015), pp. 1147–1168.

[12] S. X. GAO, H. J. XU AND Y. C. BAI, *Theoretical analyses on bed topography responses in large depth-to-width ratio river bends with constant curvatures*, J. Appl. Math. Mech., 39 (2018), pp. 747–766.

[13] P. A. NELSON, M. B. PITTALUGA AND G. SEMINARA, *Finite amplitude bars in mixed bedrock-alluvial channels*, J. Geophys. Res. Earth Surf., 119 (2014), pp. 566–587.

[14] H. ZHOU, AND X. Y. YOU, *On the weakly nonlinear thoery in dydrodynamic stability*, Sci. Sin., Ser. A (Engl. Ed.), 6 (1992), pp. 615–622.

[15] X. S. WU, S. SOOLEE AND Y. J. COWLEY, *On the weakly nonlinear three-dimensional instability of shear layers to pairs of oblique waves: the Stokes layer as a paradigm*, J. Fluid Mech., 253 (1993), pp.681–721.

[16] J. T. STUART, *On the non-linear mechanics of wave disturbances in stable and unstable parallel flows. Part 1. The basic behaviour in plane Poiseuille flow*, J. Fluid Mech., 3 (1960), pp. 353–370.

[17] Z. HENG AND K. FUJIMURA, *Further improvement of weakly nonlinear theory of hydrodynamic stability*, Sci. Sin., Ser. A (Engl. Ed.), 1 (1998), pp. 84–92.

[18] L. Y. SHEN, C. G. LU, W. G. WU AND S. F. XUE, *A high-order numerical study three-dimensional hydrodynamics in a natural river*, Adv. Appl. Math. Mech., 7 (2015), pp. 180–195.

[19] J. D. SMITH AND S. R. MCLEAN, *A model for flow in meandering streams*, Water Resour. Res., 20 (1984), pp. 1301–1315.

[20] P. F. ZACHMANN AND W. LAGASSE, Handbook for Predicting Stream Meander Migration, Transportation Research Board, Washington, (2004).
[21] X. S. WU, *Nonlinear theories for shear flow instabilities: physical insights and practical implications*, Annu. Rev. Fluid Mech., 51 (2019), pp. 451–485.
[22] M. NISHIOKA, A. S. LID AND Y. ICHIKAWA, *An experimental investigation of the stability of plane Poiseuille flow*, J. Fluid Mech., 72 (1975), pp. 731–751.
[23] S. A. ORSZAG, *Accurate solution of the Orr–Sommerfeld stability equation*, J. Fluid Mech., 50 (1971), pp. 689–703.
[24] Y. C. BAI, Z. Q. JI AND H. J. XU, *Stability and self-adaption character of turbulence coherent structure in narrow-deep river bend*, Sci. China Technol. Sci., 55 (2012), pp. 2990–2999.